Original Article

Differentiation between pancreatic metastases from renal cell carcinoma and pancreatic neuroendocrine neoplasm using endoscopic ultrasound

Kunio Kataoka[1], MD, Takuya Ishikawa[1], MD, PhD, Eizaburo Ohno[1], MD, PhD, Yasuyuki Mizutani[1], MD, PhD, Tadashi Iida[1], MD, Eri Ishikawa[1], MD, PhD, Kazuhiro Furukawa[1], MD, PhD, Masanao Nakamura[1], MD, PhD, Takashi Honda[1], MD, PhD, Masatoshi Ishigami[1], MD, PhD, Hiroki Kawashima[2], MD, PhD, Yoshiki Hirooka[3], MD, PhD, Mitsuhiro Fujishiro[1], MD, PhD

1. Department of Gastroenterology and Hepatology, Nagoya University Graduate School of Medicine, Nagoya, Japan

2. Department of Endoscopy, Nagoya University Hospital, Nagoya, Japan

3. Department of Gastroenterology and Gastroenterological Oncology, Fujita Health University, Toyoake, Japan

Corresponding author: Hiroki Kawashima

E-mail: h-kawa@med.nagoya-u.ac.jp

ADDRESS: 65 Tsurumai-cho, Showa-ku, Nagoya, 466-8550, Japan

TEL.: +81-52-744-2602, FAX: +81-52-744-2785

Author Contributions

Conception and design: Kataoka K, Ishikawa T, Kawashima H, Ohno E

Analysis and interpretation of the data: Kataoka K, Ishikawa T, Kawashima H, Ohno E, Ishikawa E

Drafting of the article: Kataoka K, Ishikawa T, Kawashima H, Ohno E, Mizutani Y, Iida T, Ishikawa E, Furukawa K, Nakamura M, Honda T, Ishigami M, Hirooka Y

Critical revision of the article for important intellectual content: Fujishiro M

Final approval of the article: All authors

Differentiation between pancreatic metastases from renal cell carcinoma and pancreatic neuroendocrine neoplasm using endoscopic ultrasound

ABSTRACT

Objectives: Pancreatic metastases from renal cell carcinoma (PRCC) often appear many years after treatment of the primary tumor, and differentiation from pancreatic neuroendocrine neoplasm (PanNEN) can be challenging due to their hypervascularity. Here, we investigated the utility of endoscopic ultrasound (EUS) for differentiation of these conditions.

Methods: A retrospective analysis was performed in 17 and 79 consecutive patients with pathologically proven PRCC and non-functional PanNEN who were examined by EUS. In cases examined by EUS elastography or contrast-enhanced harmonic EUS (CH-EUS), the lesions were classified as stiff or soft, or into three vascular patterns as hypoechoic, isoechoic, and hyperechoic. CH-EUS images at 20 s, 40 s, 60 s, 3 min and 5 min were used for evaluation. EUS images were independently reviewed by two readers who were blinded to all clinical information.

Results: The patients with PRCC were significantly older than those with PanNEN (median, 71 (range, 45-81) vs. 58 (22-76), $P = 0.001$) and more often had multiple tumors (6/17 (35%) vs. 7/79 (9%), $P = 0.010$). In EUS findings, PRCC lesions significantly more frequently had a marginal hypoechoic zone (MHZ) (11/17 (65%) vs. 27/79 (34%), $P = 0.028$), being classified as soft (12/13 (92%) vs. 26/58 (45%), $P = 0.002$),

and showed sustained hyperechoic vascular patterns at 5 min (7/8 (88%) vs. 4/59 (7%), $P < 0.001$) compared to PanNEN lesions.

Conclusions: The presence of a MHZ, a soft lesion, and a sustained hyperechoic vascular pattern in EUS may be useful for differentiating PRCC from PanNEN.

Introduction

Pancreatic metastases are most frequently derived from renal cell carcinoma (RCC) [1, 2] and these metastases (referred to as PRCC) typically show hypervascularity in contrast-enhanced CT (CE-CT) or MRI [3-5]. This observation can overlap with that for pancreatic neuroendocrine neoplasm (PanNEN), which also usually shows hypervascularity [3]. Multiple pancreatic masses may appear in PRCC and PanNEN, and this occurs at increased frequency in patients with a variety of genetic syndromes, including Von Hippel-Lindau disease [6]. Distinction of PRCC from PanNEN is further complicated by the pancreas often being the only site of RCC metastasis, and PRCC also commonly presents as a solitary mass many years after treatment of the primary tumor [3, 7, 8].

It is clinically important to differentiate PRCC from PanNEN before treatment because the therapeutic options and prognoses differ. PRCC is resected if possible [3, 9, 10], whereas, although surgery is generally recommended for PanNEN, a “wait and watch” strategy is an option for lesions of <20 mm, pancreatic neuroendocrine tumor (PanNET) G1, and non-functional tumors without visible metastasis, given the morbidity of pancreatectomy [11-13]. Systemic treatment can also be considered for PRCC in non-surgical candidates, and for advanced PanNEN [14, 15].

In general, histological sampling is desired before initiation of definitive therapy and is performed using endoscopic ultrasound-guided fine needle aspiration (EUS-FNA). However, this procedure is invasive and may not lead to a diagnosis for pancreatic masses, including in up to 21% of PanNEN cases [16]. Accurate

differentiation between PRCC and PanNEN using imaging could eliminate the need for histological sampling to confirm diagnosis, especially in cases in which surgery is being considered. In endoscopic ultrasound (EUS), the morphology of PRCC and PanNEN are similar [3, 17]. However, the utility of EUS elastography (EUS-EG) and contrast-enhanced harmonic EUS (CH-EUS) [18, 19] has not been examined in this setting. Therefore, the purpose of this study was to explore the value of EUS findings for differentiating PRCC from PanNEN.

Methods

Study design

A single-center retrospective study was performed at Nagoya University Hospital after approval by the hospital Ethics Committee (date registered: December 8, 2015, approval number: 2015-0316).

Patients

Patients with PRCC and PanNEN examined by EUS and pathologically diagnosed by surgical resection or EUS-FNA between May 2005 and September 2019 were identified in the hospital database. PanNEN was limited to non-functional lesions because differentiation of functional lesions from PRCC is not a problem. Only the largest lesion was analyzed in patients with multiple tumors. The pathology of the PanNEN group was classified based on the WHO classification [20].

Conventional EUS

EUS was performed by three experts with experience of ≥10 years (YH, EO, and TI) or trainees under their supervision. Vital signs were monitored in the left lateral position under sedation with midazolam. Various echoendoscopes and ultrasound observation systems were used, with the selection of the scope and system left to the discretion of the experts. EUS images were saved as still images. In the Japan Society of Ultrasonics in Medicine [21], conventional EUS findings of predetermined tumor characteristics (tumor contour [clear and irregular/clear and regular/unclear] and interior [hyper/iso/hypoechoic], and the presence of a marginal hypoechoic zone (MHZ, Figure 1), a lateral shadow (LS), anechoic areas, or calcification echoes) are defined. EUS images were investigated based on these definitions. As for color or power Doppler imaging (CDI), based on the previous report of vascular architecture (VA) classification [22], the images were classified into type A (peritumoral with or without intratumoral vessels [A2 or A1]); type B (only intratumoral vessels); and type C (flow was absent) (Figure 1).

EUS-EG

After conventional EUS, strain elastography was performed using a Real-time Tissue Elastography (Hitachi, Tokyo, Japan), ELST (Olympus, Tokyo, Japan) or Elastography (Fujifilm, Tokyo, Japan) system. The region of interest (ROI) was set to include the whole lesion with a sufficient surrounding area, such

that the lesion occupied <50% of the whole ROI. Strain elastography was used to estimate relative tissue stiffness based on the distortion generated by an aortic pulse. For relative tissue elasticities (stiffness) of stiff, average and soft, tissues were visualized as blue, green and red, respectively (Figure 2, 3). Since the EUS-EG color map changes rapidly, a video was acquired for several seconds and still images of the lesion were extracted from the video. This procedure was repeated multiple times, as needed. With reference to our previous study [23], each EUS-EG image was classified as blue-dominant, equivalent, or green-dominant based on the blue: green ratio in the lesion. Using multiple EUS-EG images from the same patient, a lesion with a greater number of blue-dominant than green-dominant images was classified as stiff, and all other lesions were defined as soft. Since this was a retrospective study, EUS-EG was not performed in some cases.

CH-EUS

In CH-EUS, one vial of Sonazoid (16 ml as perflubutane) (Daiichi-Sankyo, Tokyo, Japan) was suspended in 2 ml of water for injection, and the suspension was administered by bolus injection at 0.015 ml/kg. After Sonazoid injection, CH-EUS images were recorded as a movie for 60 s continuously, and images at 3 and 5 min were also recorded. The stored data were used for analysis. Images at 20 s, 40 s, 60 s, 3 min and 5 min were used for evaluation. Based on our previous study [24], the images were classified into three patterns, as hyperechoic, isoechoic, or hypoechoic vascular, compared with the surrounding pancreatic

parenchyma (Figure 2, 3). Since this was a retrospective study, some cases did not have images stored for each time phase in CH-EUS.

EUS-FNA

EUS-FNA was performed with linear echoendoscopes connected to an ultrasound scanning system and either 22- or 25-gauge FNA needles, with the selection of these left to the discretion of the experts. The acquired samples were assessed to provide histological and cytological diagnoses by experienced pathologists. Positive diagnosis of PRCC or PanNEN was defined as either definite or suspicious of PRCC or PanNEN. In our institution, as a rule, EUS- FNA was not performed for solid pancreatic lesions that were going to be surgically resected based on imaging findings.

Data analysis and statistics

EUS images were independently reviewed by two readers (KK and TI) who were blinded to the patient history and clinical, radiologic, histologic, and surgical information. Still images were used for evaluation. Interobserver variability of EUS findings was assessed by calculating the kappa coefficient after the two readers had made their individual assessments. Agreement was defined as minor (kappa coefficient, 0.01-0.20), fair (0.21-0.40), moderate (0.41-0.60), good (0.61-0.80), or excellent (0.81–1.00), beyond chance. The readers reassessed images that yielded discrepant findings together to reach an agreement.

For comparison between two groups, Fisher's exact test or the chi-squared test was used for categorical variables and the Mann-Whitney U test for continuous variables, with $P < 0.05$ regarded as significant. For significant EUS findings, the sensitivity, specificity, positive predictive value (PPV), negative predictive value (NPV), and accuracy for diagnosis were calculated, with the 95% confidence interval (CI) determined using the Clopper-Pearson method. For significant EUS findings, the statistical power was also calculated. All analyses were performed using SPSS Statistics v. 27.0 (SPSS, Chicago, IL, USA).

Results

Patient and lesion characteristics

The subjects were 17 and 79 consecutive patients with PRCC and non-functional PanNEN who underwent EUS as part of the initial examination. The characteristics of the patients and lesions are summarized in Table 1. There were no significant differences in gender, location, tumor size, main pancreatic duct or common bile duct dilatation due to the tumor, and distant metastasis between the PRCC and PanNEN groups. However, the patients with PRCC were significantly older (median, 71 (range, 45-81) vs. 58 (22-76) years, $P = 0.001$) and more often had multiple tumors (6/17 (35%) vs. 7/79 (9%), $P = 0.010$).

CT was performed in all cases in both PRCC and PanNEN, but only plain CT was performed in 2 cases in PRCC and 3 cases in PanNEN. CE-CT could not be performed because of renal failure in 3 cases and a

history of iodine contrast medium allergy in 2 cases. MRI was performed in 6 cases in PRCC and 30 cases in PanNEN, of which 12 cases in PanNEN were contrast-enhanced MRI. In the experts reading of CT and MRI for PRCC cases, the primary differential diagnosis was PRCC in 11 cases (65%), PanNEN in 1 case (6%), and differentiation from PanNEN or other tumors was difficult in 5 cases (29%). For PanNEN cases, the primary differential diagnosis was PanNEN in 52 cases (66%), differentiation from other tumors was difficult in 24 cases (30%), and the remaining 3 cases (4%) could not be visualized.

PRCC lesions were diagnosed by surgery in 13 cases and by EUS-FNA only in the remaining 4 cases; PanNEN lesions were diagnosed by surgery in 73 cases and by biopsy only, such as EUS-FNA, in the remaining 6 cases.

All the primary RCCs were the clear cell type. The median time to recurrence of PRCC after initial nephrectomy was 13 years (range, 1-23 years). Of the 17 patients with PRCC, 15 had no extrapancreatic metastatic lesions at the time of diagnosis of PRCC, one had right gluteus maximus muscle metastasis, and one had lung metastasis.

In the PanNEN group, 57 lesions (72%) were classified as PanNET G1, 13 (16%) as PanNET G2, and 1 (1%) as PanNET G3 according to the WHO classification [20]. The classification of the 8 other lesions (10%) was unknown because they were diagnosed by biopsy or Ki-67 staining was not performed. Regarding hereditary disease, 2 patients had Von Hippel-Lindau disease and 2 had multiple endocrine neoplasia type 1.

Conventional EUS

There were no significant differences between PRCC and PanNEN in tumor contour and interior, and the presence of a LS, anechoic area, or calcification echoes, and most of the cases were visualized as a hypoechoic lesion with a clear and regular contour (Figure 1-3). Among conventional EUS findings, only the presence of a MHZ differed significantly between the groups (Table 2), with PRCC lesions having a MHZ significantly more often (11/17 (65%) vs. 27/79 (34%), $P = 0.028$). Regarding VA classification of CDI, there was no significant difference between PRCC and PanNEN cases, but PRCC lesions tended to be classified as type A2 (type A1/A2/B/C, 5/8/2/1 vs. 24/15/17/18, $P = 0.064$) (Table 2).

EUS-EG

EUS-EG was performed for 13 PRCC cases and 58 PanNEN cases (Table 2). The PRCC lesions were significantly more often classified as soft compared to PanNEN lesions (12/13 (92%) vs. 26/58 (45%), P = 0.002).

CH-EUS

In CH-EUS (Table 3), at 20 s all 10 PRCC lesions showed hyperechoic vascular patterns, whereas of the 63 PanNEN lesions, 43, 17, and 3 had hyper, iso, and hypoechoic vascular patterns, respectively, with no

significant difference between the groups (P = 0.112). After 40 s, significant differences were observed, and at 5 min, of the 8 evaluable PRCC lesions, 7 had hyper and 1 had isoechoic vascular patterns, whereas of the 59 PanNEN lesions, 4, 22, and 33 had hyper, iso, and hypoechoic vascular patterns. The frequency of hyperechoic vascular patterns at 5 min showed the largest significant difference. These results show that PRCC lesions gave more sustained hyperechoic vascular patterns.

Differentiation between PRCC and PanNET G1 or G2/G3

Among conventional EUS findings between PRCC and PanNET G1, in addition to the presence of a MHZ, VA classification of CDI also showed a significant difference. On the other hand, between PRCC and PanNET G2/G3, the presence of a MHZ did not show a significant difference, but the presence of calcification echoes differed significantly, with PanNET G2/G3 lesions having calcification echoes significantly more often (7/14 (50%) vs. 1/17 (6%), P = 0.011). In EUS-EG, the PRCC lesions were significantly more often classified as soft compared to PanNET G1 or G2/G3 lesions (Table 2). In CH-EUS, unlike PanNET G1, between PRCC and PanNET G2/G3, there were significant differences in all time points including at 20 s (Table 3).

EUS-FNA

EUS-FNA was performed in a total of 13 cases for PRCC and 15 cases for PanNEN, and positive

diagnoses were obtained in 9 (69%) and 10 (67%) cases, respectively, with no significant difference (P = 1.000).

Diagnostic values

MHZ in conventional EUS, the pattern classification in EUS-EG, and CH-EUS gave significant findings. The diagnostic values of these findings are shown in Table 4. In the entire population (n=96), the sensitivity, specificity, and accuracy of MHZ presence for diagnosis of PRCC were 65% (95% CI: 38%-86%), 66% (54%-76%), and 66% (55%-75%), respectively. In patients examined by EUS-EG (n=71), these parameters for use of a soft lesion for diagnosis of PRCC were 92% (64%-100%), 55% (42%-68%), and 62% (50%-73%), respectively; and in patients with a CH-EUS image at 5 min (n=67), the same parameters for use of a hyperechoic vascular pattern for diagnosis of PRCC were 88% (48%-100%), 93% (84%-98%), and 93% (83%-98%), respectively. All three of these findings had high NPV but unsatisfactory PPV. As for the statistical power, the presence of a MHZ was low at 0.548, but a soft lesion in EUS-EG and the presence of sustained hyperechoic vascular patterns in CH-EUS was high at 0.873 and 0.994, respectively.

Analyses of interobserver agreement

Kappa coefficients showed that interobserver agreement evaluated by two readers was all good for conventional EUS findings (kappa coefficient = 0.639–0.732), the pattern classification in EUS-EG (kappa

coefficient = 0.745) (Table 2), and CH-EUS findings (kappa coefficient = 0.723-0.793) (Table 3).

Discussion

PRCC and PanNEN are hypervascular tumors, and PRCC often appears as a solitary pancreatic mass a long time after resection of the primary tumor, and thus requires differentiation from PanNEN [3-5, 7, 8]. Although CT is considered particularly important for differentiating between the two due to its versatility, its diagnostic ability is not sufficient because not all cases can be contrast-enhanced, small lesions may not be visualized, and the positive diagnosis rate at our institution was less than 70%. EUS-FNA is important, especially in non-resected cases, but it is uncertain, and the positive diagnosis rate at our institution was less than 70%. The results of this study showed that PRCC lesions significantly more often had a MHZ in conventional EUS, were significantly more often classified as a soft lesion in EUS-EG, and showed significantly more sustained hyperechoic vascular patterns in CH-EUS. These findings may be complementary to the diagnostic ability of CT and EUS-FNA.

In this study, PRCC and PanNEN showed similar appearance in conventional EUS and they were often visualized as a hypoechoic lesion with a clear and regular contour, as previously reported [3]. The only significant difference was in the frequency of presence of a MHZ, which was more common in PRCC (11/17 cases, 65%). This may reflect the thick fibrous coat and may be one of the pathological features of PRCC, but its diagnostic value was not high and its clinical utility was limited to PanNET G1. On the other

hand, for PanNET G2/G3, there was a significant difference only in the presence of calcification echoes. Regarding VA classification of CDI, it has been reported that PanNET G1 is often classified as type A1, G2 as type B, and G3 as type C [22]. In this study, G1 was also most commonly classified as type A1, G2 as type B. PRCC was most commonly classified as type A2, which may suggest more blood flow than PanNEN, although there was no significant difference.

In EUS-EG, PRCC lesions were classified as soft in 12 of 13 cases (92%), which was significantly more than that for PanNEN lesions (26/58 cases, 45%). There are few reports of use of EUS-EG in PanNEN cases, but soft lesions have been found in 73/114 cases (64%) with lesions of ≤15 mm [25], and in our previous study of lesions of ≤20 mm, 17/31 (55%) were soft lesions [23]. Iglesias-Garcia et al. classified 10/10 cases (100%) as having a homogenous blue pattern; i.e., a stiff lesion [26]. PanNEN lesions seems to be able to appear as both stiff and soft, and fibrosis may increase in more malignant lesions [27], which may influence the stiff-soft heterogeneity. On the other hand, the pathology of clear cell RCC is characterized by a high intracellular lipid content [28, 29]. PRCC, which generally occurs only in clear cell RCC, has also been inferred to be lipid-rich based on MRI [30], which may be related to the tendency of PRCC lesions to appear as soft in EUS-EG.

In CH-EUS, 7 of 8 PRCC (88%) cases had sustained hyperechoic vascular patterns until 5 min, which was significantly more than the 4 of 59 PanNEN cases (7%). PanNEN generally shows hypervascularity in CH-EUS, but this has been reported mostly up to around 60 s [24, 27, 31]. In this study, PanNEN lesions

showed a decrease in contrast effect over time at 3 min and 5 min, and the differences between PanNEN and PRCC increased. CH-EUS images are thought to reflect the density and distribution of microvascular and fibrous tissue [24, 27], and this may also influence the difference in images between PRCC and PanNEN. That is, PRCC lesions, which are pathologically characterized by an abundance of capillaries [32], may have more microvascular and less fibrous tissue than PanNEN lesions. Kang et al. found that in CE-CT, PRCC had significantly more hypervascularity in the arterial phase than PanNEN, and then significantly washed out [4]. Unlike ultrasound contrast medium, iodine contrast medium migrates from the intravascular region to the stroma over time, and these CE-CT findings may support the view of more microvascular and less fibrous tissue in PRCC lesions.

In recent years, somatostatin receptor scintigraphy such as ^{111}In-octreoscan, ^{68}Ga-DOTATOC- PET/CT, or ^{68}Ga-DOTATATE-PET/CT can be used to detect PanNEN. These techniques are dependent on cell surface expression of somatostatin receptors, which is not always high particularly in poorly differentiated PanNEN lesions and are known to have several other pitfalls [33]. ^{111}In-octreoscan has been reported to have a sensitivity of 52%, specificity of 93%, and accuracy of 58%, which is high specificity but not necessarily high sensitivity [34]. Furthermore, some RCC lesions express somatostatin receptors and can be detected by somatostatin receptor scintigraphy [35], which make complicate to differentiate PRCC from PanNEN.

The limitations of this study include its retrospective single-center design; the small number of patients,

particularly for PRCC cases; the long study period and the use of various echoendoscopes and ultrasound apparatuses; not all cases underwent EUS-EG and CH-EUS, and not all CH-EUS images for each time phase were stored; and not all cases were diagnosed by surgery. However, a long study period and the inclusion of cases using various echoendoscopes and ultrasound apparatuses are required to increase the number of PRCC cases, which are quite rare. Future larger scale studies are needed to validate our results.

In conclusion, among EUS findings, the presence or absence of a MHZ, the pattern classification in EUS-EG, and the presence or absence of sustained hyperechoic vascular patterns in CH-EUS may be useful in differentiating PRCC from non-functional PanNEN.

References

[1] Adsay NV, Andea A, Basturk O, Kilinc N, Nassar H, Cheng JD. Secondary tumors of the pancreas: an analysis of a surgical and autopsy database and review of the literature. Virchows Arch 2004; 444: 527-35.

[2] Masetti M, Zanini N, Martuzzi F, Fabbri C, Mastrangelo L, Landolfo G, et al. Analysis of prognostic factors in metastatic tumors of the pancreas: a single-center experience and review of the literature. Pancreas 2010; 39: 135-43.

[3] Ballarin R, Spaggiari M, Cautero N, De Ruvo N, Montalti R, Longo C, et al. Pancreatic metastases from renal cell carcinoma: the state of the art. World J Gastroenterol 2011; 17: 4747-56.

[4] Kang TW, Kim SH, Lee J, Kim AY, Jang KM, Choi D, et al. Differentiation between pancreatic

metastases from renal cell carcinoma and hypervascular neuroendocrine tumour: Use of relative percentage washout value and its clinical implication. Eur J Radiol 2015; 84: 2089-96.

[5] van der Pol CB, Lee S, Tsai S, Larocque N, Alayed A, Williams P, et al. Differentiation of pancreatic neuroendocrine tumors from pancreas renal cell carcinoma metastases on CT using qualitative and quantitative features. Abdom Radiol (NY) 2019; 44: 992-9.

[6] Taouli B, Ghouadni M, Corréas JM, Hammel P, Couvelard A, Richard S, et al. Spectrum of abdominal imaging findings in von Hippel-Lindau disease. AJR Am J Roentgenol 2003; 181: 1049-54.

[7] Kassabian A, Stein J, Jabbour N, Parsa K, Skinner D, Parekh D, et al. Renal cell carcinoma metastatic to the pancreas: a single-institution series and review of the literature. Urology 2000; 56: 211-5.

[8] Sellner F, Tykalsky N, De Santis M, Pont J, Klimpfinger M. Solitary and multiple isolated metastases of clear cell renal carcinoma to the pancreas: an indication for pancreatic surgery. Ann Surg Oncol 2006; 13: 75-85.

[9] Sperti C, Moletta L, Patanè G. Metastatic tumors to the pancreas: The role of surgery. World J Gastrointest Oncol 2014; 6: 381-92.

[10] Schwarz L, Sauvanet A, Regenet N, Mabrut JY, Gigot JF, Housseau E, et al. Long-term survival after pancreatic resection for renal cell carcinoma metastasis. Ann Surg Oncol 2014; 21: 4007-13.

[11] Lee LC, Grant CS, Salomao DR, Fletcher JG, Takahashi N, Fidler JL, et al. Small, nonfunctioning, asymptomatic pancreatic neuroendocrine tumors (PNETs): role for nonoperative management. Surgery

2012; 152: 965-74.

[12] Rosenberg AM, Friedmann P, Del Rivero J, Libutti SK, Laird AM. Resection versus expectant management of small incidentally discovered nonfunctional pancreatic neuroendocrine tumors. Surgery 2016; 159: 302-9.

[13] Falconi M, Eriksson B, Kaltsas G, Bartsch DK, Capdevila J, Caplin M, et al. ENETS Consensus Guidelines Update for the Management of Patients with Functional Pancreatic Neuroendocrine Tumors and Non-Functional Pancreatic Neuroendocrine Tumors. Neuroendocrinology 2016; 103: 153-71.

[14] Dutcher JP. Recent developments in the treatment of renal cell carcinoma. Ther Adv Urol 2013; 5: 338-53.

[15] Raymond E, Dahan L, Raoul JL, Bang YJ, Borbath I, Lombard-Bohas C, et al. Sunitinib malate for the treatment of pancreatic neuroendocrine tumors. N Engl J Med 2011; 364: 501-13.

[16] Bernstein J, Ustun B, Alomari A, Bao F, Aslanian HR, Siddiqui U, et al. Performance of endoscopic ultrasound-guided fine needle aspiration in diagnosing pancreatic neuroendocrine tumors. Cytojournal 2013; 10: 10. doi: 10.4103/1742-6413.112648.

[17] Pannala R, Hallberg-Wallace KM, Smith AL, Nassar A, Zhang J, Zarka M, et al. Endoscopic ultrasound-guided fine needle aspiration cytology of metastatic renal cell carcinoma to the pancreas: A multi-center experience. Cytojournal 2016; 13: 24. doi: 10.4103/1742-6413.192191.

[18] Hirooka Y, Itoh A, Kawashima H, Ohno E, Ishikawa T, Matsubara H, et al. Diagnosis of pancreatic

disorders using contrast-enhanced endoscopic ultrasonography and endoscopic elastography. Clin Gastroenterol Hepatol 2009; 7: 63-7.

[19] Ohno E, Kawashima H, Hashimoto S, Goto H, Hirooka Y. Current status of tissue harmonic imaging in endoscopic ultrasonography (EUS) and EUS-elastography in pancreatobiliary diseases. Dig Endosc 2015; 27: 68-73.

[20] Lloyd RV, Osamura RY, Klöppel G, et al. WHO classification of tumours of endocrine organs, 4th edn. International Agency for Research on Cancer, Lyon, 2017.

[21] Terminology and Diagnostic Criteria Committee, Japan Society of Ultrasonics in Medicine. Ultrasonographic diagnostic criteria for pancreatic cancer. J Med Ultrason (2001) 2013; 40: 497-504.

[22] Chen K, Zhang W, Zhang Z, He Y, Liu Y, Yang X. Simple Vascular Architecture Classification in Predicting Pancreatic Neuroendocrine Tumor Grade and Prognosis. Dig Dis Sci 2018; 63: 3147-52.

[23] Kataoka K, Ishikawa T, Ohno E, Iida T, Suzuki H, Uetsuki K, et al. Endoscopic ultrasound elastography for small solid pancreatic lesions with or without main pancreatic duct dilatation. Pancreatology 2021; 21: 451-8.

[24] Ishikawa T, Hirooka Y, Kawashima H, Ohno E, Hashizume K, Funasaka K, et al. Multiphase evaluation of contrast-enhanced endoscopic ultrasonography in the diagnosis of pancreatic solid lesions. Pancreatology 2018; 18: 291-7.

[25] Ignee A, Jenssen C, Arcidiacono PG, Hocke M, Möller K, Saftoiu A, et al. Endoscopic ultrasound

elastography of small solid pancreatic lesions: a multicenter study. Endoscopy 2018; 50: 1071-9.

[26] Iglesias-Garcia J, Larino-Noia J, Abdulkader I, Forteza J, Dominguez-Munoz JE. EUS elastography for the characterization of solid pancreatic masses. Gastrointest Endosc 2009; 70: 1101-8.

[27] Palazzo M, Napoléon B, Gincul R, Pioche M, Pujol B, Lefort C, et al. Contrast harmonic EUS for the prediction of pancreatic neuroendocrine tumor aggressiveness (with videos). Gastrointest Endosc 2018; 87: 1481-8.

[28] Reuter VE. The pathology of renal epithelial neoplasms. Semin Oncol 2006; 33: 534-43.

[29] Reuter VE, Tickoo SK. Differential diagnosis of renal tumours with clear cell histology. Pathology 2010; 42: 374-83.

[30] Lyu HL, Cao JX, Wang HY, Wang ZB, Hu MG, Ma L, et al. Differentiation between pancreatic metastases from clear cell renal cell carcinoma and pancreatic neuroendocrine tumor using double-echo chemical shift imaging. Abdom Radiol (NY) 2018; 43: 2712-20.

[31] Kitano M, Kudo M, Yamao K, Takagi T, Sakamoto H, Komaki T, et al. Characterization of small solid tumors in the pancreas: the value of contrast-enhanced harmonic endoscopic ultrasonography. Am J Gastroenterol 2012; 107: 303-10.

[32] Cheng SK, Chuah KL. Metastatic Renal Cell Carcinoma to the Pancreas: A Review. Arch Pathol Lab Med 2016; 140: 598-602.

[33] Hofman MS, Lau WF, Hicks RJ. Somatostatin receptor imaging with 68Ga DOTATATE PET/CT:

clinical utility, normal patterns, pearls, and pitfalls in interpretation. Radiographics 2015; 35: 500-16.

[34] Gabriel M, Decristoforo C, Kendler D, Dobrozemsky G, Heute D, Uprimny C, et al. 68Ga-DOTA-Tyr3-octreotide PET in neuroendocrine tumors: comparison with somatostatin receptor scintigraphy and CT. J Nucl Med 2007; 48: 508-18.

[35] Freudenberg LS, Gauler T, Görges R, Bauer S, Stergar H, Antoch G, et al. Somatostatin receptor scintigraphy in advanced renal cell carcinoma. Results of a phase II-trial of somatostatine analogue therapy in patients with advanced RCC. Nuklearmedizin 2008; 47: 127-31.

Figure legends

Figure 1: (a) A pancreatic metastases from renal cell carcinoma (PRCC) case. Endoscopic ultrasound (EUS) showed a 10-mm hypoechoic lesion with a clear and regular contour that did not have a marginal hypoechoic zone (MHZ). This lesion was classified as type A1 by vascular architecture (VA) classification. (b) A PRCC case. EUS showed a 26-mm isoechoic lesion with a clear and regular contour that had a MHZ. This lesion was classified as type A2 by VA classification. (c) A pancreatic neuroendocrine tumor (PanNET) G3 case. EUS showed a 36-mm hypoechoic lesion with a clear and regular contour that did not have a MHZ. This lesion was classified as type B by VA classification. (d) A PanNET G1 case. EUS showed a 22-mm hypoechoic lesion with a clear and regular contour that had a MHZ. This lesion was classified as type C by VA classification. The echoendoscope and ultrasound apparatus used were a combination of GF-UCT260 (Olympus, Tokyo, Japan) with ARIETTA 850 (Hitachi, Tokyo, Japan) for (a) and (b), EG-3670URK (Pentax, Tokyo, Japan) with HiVision Ascendus (Hitachi) for (c), and GF-UE260-AL5 (Olympus) with Prosound α-10 (Hitachi) for (d).

Figure 2: A pancreatic metastases from renal cell carcinoma (PRCC) case. The patient was a 59-year-old woman. Postoperative follow-up CT for left renal cell carcinoma 13 years after treatment showed a pancreatic tail mass. Endoscopic ultrasound (EUS) showed a 32-mm isoechoic lesion with a clear and regular contour that had a marginal hypoechoic zone (a). EUS-elastography gave green-dominant patterns and the lesion was classified as soft (b). In contrast-enhanced harmonic EUS, the lesion had a hyperechoic

vascular pattern at 20 s that persisted up to 60 s, after which there was a decrease in the contrast effect over time, but the hyperechoic pattern persisted even after 3 min and 5 min (c). The patient underwent spleen preserving distal pancreatectomy, with histology revealing PRCC. Hematoxylin and eosin staining showed that the tumor was covered by a thick fibrous coat (d). On magnification, atypical cells with mildly enlarged atypical nuclei and pale cytoplasm formed spores compartmentalized by abundant capillaries. There were no fibrous components in the tumor (e). The echoendoscope and ultrasound apparatus used was a combination of EG-3670URK (Pentax, Tokyo, Japan) with HiVision Ascendus (Hitachi, Tokyo, Japan).

Figure 3: A pancreatic neuroendocrine tumor (PanNET) G1 case. The patient was a 49-year-old man. CE-CT performed for an enlarging renal cyst showed a pancreatic head mass. Endoscopic ultrasound (EUS) showed a 9-mm hypoechoic lesion with a clear and regular contour and no marginal hypoechoic zone. In EUS-elastography, green-dominant patterns were seen and the lesion was classified as soft (a). In contrast-enhanced harmonic EUS, the lesion showed a hyperechoic vascular pattern at 20 s, isoechoic vascular patterns at 40 s, 60 s, and 3 min, and a hypoechoic vascular pattern at 5 min (b). The patient underwent subtotal stomach-preserving pancreaticoduodenectomy, with histology revealing PanNET G1. Hematoxylin and eosin staining showed that the tumor was covered by a fibrous coat, but invaded by spores (c). On magnification, atypical cells with relatively small nucleoli and eosinophilic cytoplasm formed neuroendocrine features such as ribbon and trabecular patterns. There were some fibrous components in the tumor (d). Immunohistochemical staining was positive for chromogranin A, synaptophysin, and CD 56.

The echoendoscope and ultrasound apparatus used was a combination of GF-UCT260 (Olympus, Tokyo, Japan) with ARIETTA 850 (Hitachi, Tokyo, Japan).

Table 1: Characteristics of the patients and lesions included in this study.

	PRCC (n = 17)	PanNEN (n = 79)	*P* value
Age, median (range), years	71 (45-81)	58 (22-76)	< 0.001*
Gender			1.000**
Male	12 (71%)	43 (54%)	
Female	5 (29%)	36 (46%)	
Multiple tumors			0.010**
Yes	6 (35%)	7 (9%)	
No	11 (65%)	72 (91%)	
Location of single tumor			0.293***
Head/Body/Tail	2/5/4	30/20/22	
Size, median (range), mm	21 (9-36)	18 (7-110)	0.935*
Main pancreatic duct or common bile duct dilation			0.732**
Present	4 (24%)	14 (18%)	
Absent	13 (76%)	65 (82%)	
Metastases to other organs			1.000**
Present	2 (12%)	10 (13%)	
Absent	15 (88%)	69 (87%)	

PRCC, pancreatic metastases from renal cell carcinoma; PanNEN, pancreatic neuroendocrine neoplasm.

*Mann-Whitney U test, **Fisher's exact test, ***chi-squared test.

Table 2: Comparison of the conventional EUS findings and the EUS-EG stiffness classification between PRCC and PanNEN.

	PRCC	PanNEN	*P* value	PanNET G1	*P* value	PanNET G2/G3	*P* value	Kappa coefficient
Conventional EUS findings	n = 17	n = 79		n = 57		n = 14		
Contour			0.315*		0.348*		0.198**	0.639
Clear and regular	15 (88%)	57 (72%)		43 (75%)		9 (64%)		
Clear and irregular	2 (12%)	16 (20%)		8 (14%)		5 (36%)		
Unclear	0 (0%)	6 (8%)		6 (11%)		0 (0%)		
Marginal hypoechoic zone			0.028**		0.008**		0.724**	0.732
Present	11 (65%)	27 (34%)		15 (26%)		8 (57%)		
Absent	6 (35%)	52 (66%)		42 (74%)		6 (43%)		
Lateral shadow			0.163**		0.087**		1.000**	0.640
Present	14 (82%)	50 (63%)		33 (58%)		12 (86%)		
Absent	3 (18%)	29 (37%)		24 (42%)		2 (14%)		
Interior			0.726**		0.707**		1.000**	0.651
Hypoechoic	14 (82%)	67 (85%)		49 (86%)		11 (79%)		
Iso or hyperechoic	3 (18%)	12 (15%)		8 (14%)		3 (21%)		
Anechoic areas			0.548**		0.540**		0.233**	0.651
Present	3 (18%)	23 (29%)		15 (26%)		6 (43%)		
Absent	14 (82%)	56 (71%)		42 (74%)		8 (57%)		
Calcification echoes			0.108**		0.274**		0.011**	0.730
Present	1 (6%)	21 (27%)		11 (19%)		7 (50%)		
Absent	16 (94%)	58 (73%)		46 (81%)		7 (50%)		
CDI	n = 16	n = 74		n = 54		n = 14		
VA classification			0.064*		0.031*		0.294*	0.656
type A1	5 (31%)	24 (32%)		19 (35%)		3 (21%)		
type A2	8 (50%)	15 (20%)		9 (17%)		4 (29%)		
type B	2 (13%)	17 (23%)		9 (17%)		6 (43%)		
type C	1 (6%)	18 (24%)		17 (31%)		1 (7%)		
EUS-EG	n = 13	n = 58		n = 40		n = 13		
Stiffness classification			0.002**		0.019**		0.011**	0.745
Stiff	1 (8%)	32 (55%)		19 (48%)		10 (77%)		
Soft	12 (92%)	26 (45%)		21 (53%)		3 (23%)		

EUS, endoscopic ultrasound; EUS-EG, EUS elastography; CDI, color or power Doppler imaging; VA, vascular architecture;

PRCC, pancreatic metastases from renal cell carcinoma; PanNEN, pancreatic neuroendocrine neoplasm; PanNET, pancreatic neuroendocrine tumor.

*Chi-squared test, **Fisher's exact test.

Table 3: Comparison of the CH-EUS vascular patterns between PRCC and PanNEN.

	PRCC	PanNEN	*P* value	PanNET G1	*P* value	PanNET G2/G3	*P* value	Kappa coefficient
At 20 s	n = 10	n = 63	0.112*	n = 45	0.124*	n = 12	0.040**	0.759
Hyperechoic	10 (100%)	43 (68%)		31 (69%)		7 (58%)		
Isoechoic	0 (0%)	17 (27%)		12 (27%)		5 (42%)		
Hypoechoic	0 (0%)	3 (5%)		2 (4%)		0 (0%)		
At 40 s	n = 10	n = 59	0.014*	n = 42	0.021*	n = 11	0.022*	0.793
Hyperechoic	10 (100%)	30 (51%)		22 (52%)		5 (45%)		
Isoechoic	0 (0%)	22 (37%)		15 (36%)		5 (45%)		
Hypoechoic	0 (0%)	7 (12%)		5 (12%)		1 (9%)		
At 60 s	n = 10	n = 59	0.005*	n = 42	0.007*	n = 11	0.022*	0.783
Hyperechoic	10 (100%)	26 (44%)		19 (45%)		5 (45%)		
Isoechoic	0 (0%)	25 (42%)		17 (40%)		5 (45%)		
Hypoechoic	0 (0%)	8 (14%)		6 (14%)		1 (9%)		
At 3 min	n = 9	n = 58	< 0.001*	n = 42	< 0.001*	n = 10	< 0.001*	0.724
Hyperechoic	9 (100%)	7 (12%)		6 (14%)		0 (0%)		
Isoechoic	0 (0%)	28 (48%)		20 (48%)		5 (50%)		
Hypoechoic	0 (0%)	23 (40%)		16 (38%)		5 (50%)		
At 5 min	n = 8	n = 59	< 0.001*	n = 42	< 0.001*	n = 11	< 0.001*	0.723
Hyperechoic	7 (88%)	4 (7%)		3 (7%)		0 (0%)		
Isoechoic	1 (12%)	22 (37%)		16 (38%)		5 (45%)		
Hypoechoic	0 (0%)	33 (56%)		23 (55%)		6 (55%)		

CH-EUS, contrast-enhanced harmonic endoscopic ultrasound; PRCC, pancreatic metastases from renal cell carcinoma;

PanNEN, pancreatic neuroendocrine neoplasm; PanNET, pancreatic neuroendocrine tumor.

*Chi-squared test, **Fisher's exact test.

Table 4: Diagnostic performances of the EUS findings for differentiating PRCC from PanNEN.

	Sensitivity, % (95%CI)	Specificity, % (95%CI)	PPV, % (95%CI)	NPV, % (95%CI)	Accuracy, % (95%CI)
A marginal hypoechoic zone presence (n = 96)	65% (38%-86%)	66% (54%-76%)	29% (15%-46%)	90% (79%-96%)	66% (55%-75%)
A soft lesion in the EUS-EG stiffness classification (n = 71)	92% (64%-100%)	55% (42%-68%)	32% (18%-49%)	97% (84%-100%)	62% (50%-73%)
A hyperechoic vascular pattern at 5 min in CH-EUS (n = 67)	88% (47%-100%)	93% (84%-98%)	64% (31%-89%)	98% (91%-100%)	93% (83%-98%)

EUS, endoscopic ultrasound; PRCC, pancreatic metastases from renal cell carcinoma; PanNEN, pancreatic neuroendocrine neoplasm; CI, confidence interval;

PPV, positive predictive value; NPV, negative predictive value; EUS-EG, EUS elastography; CH-EUS, contrast-enhanced harmonic EUS.

Figure

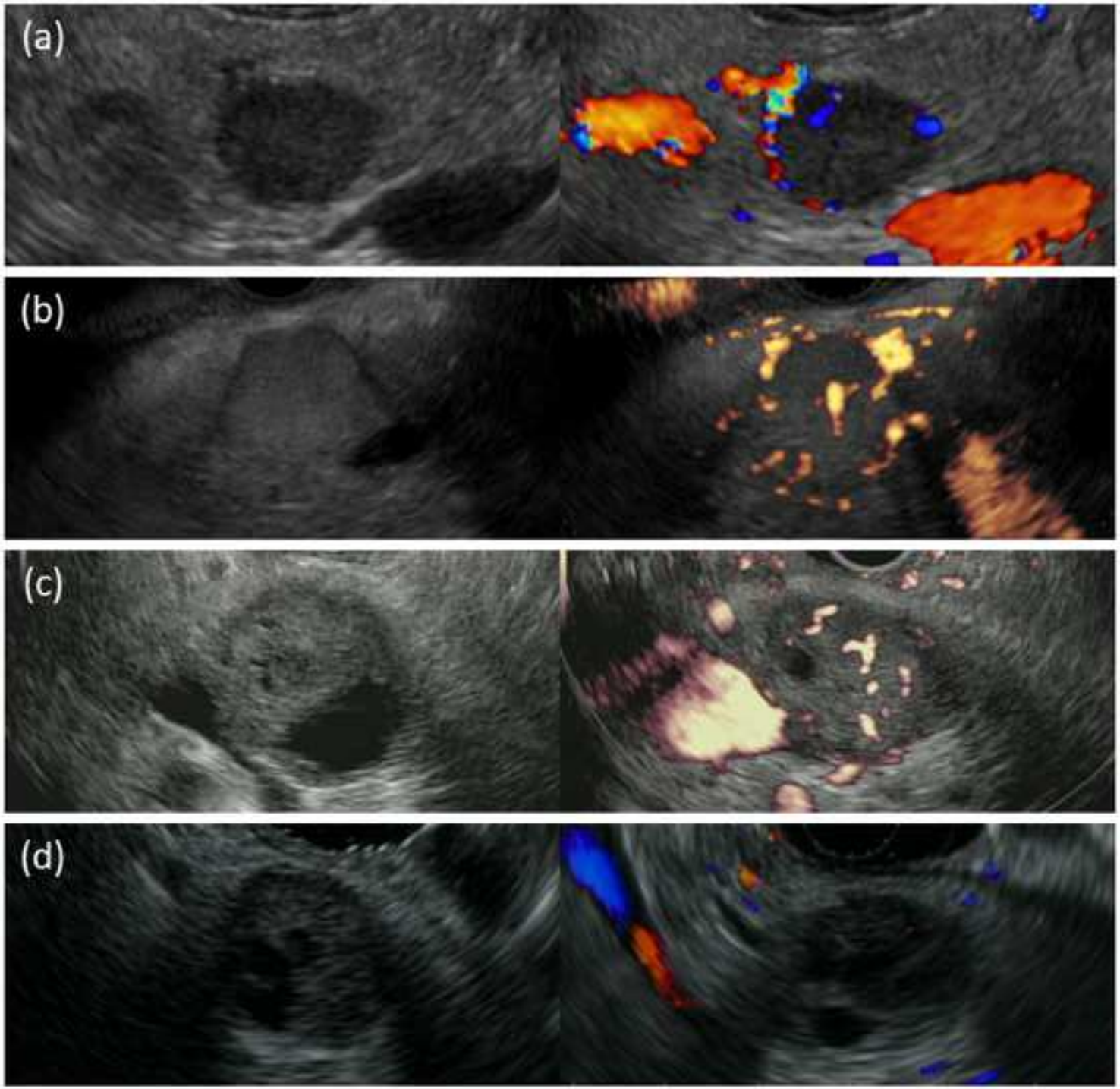

Figure

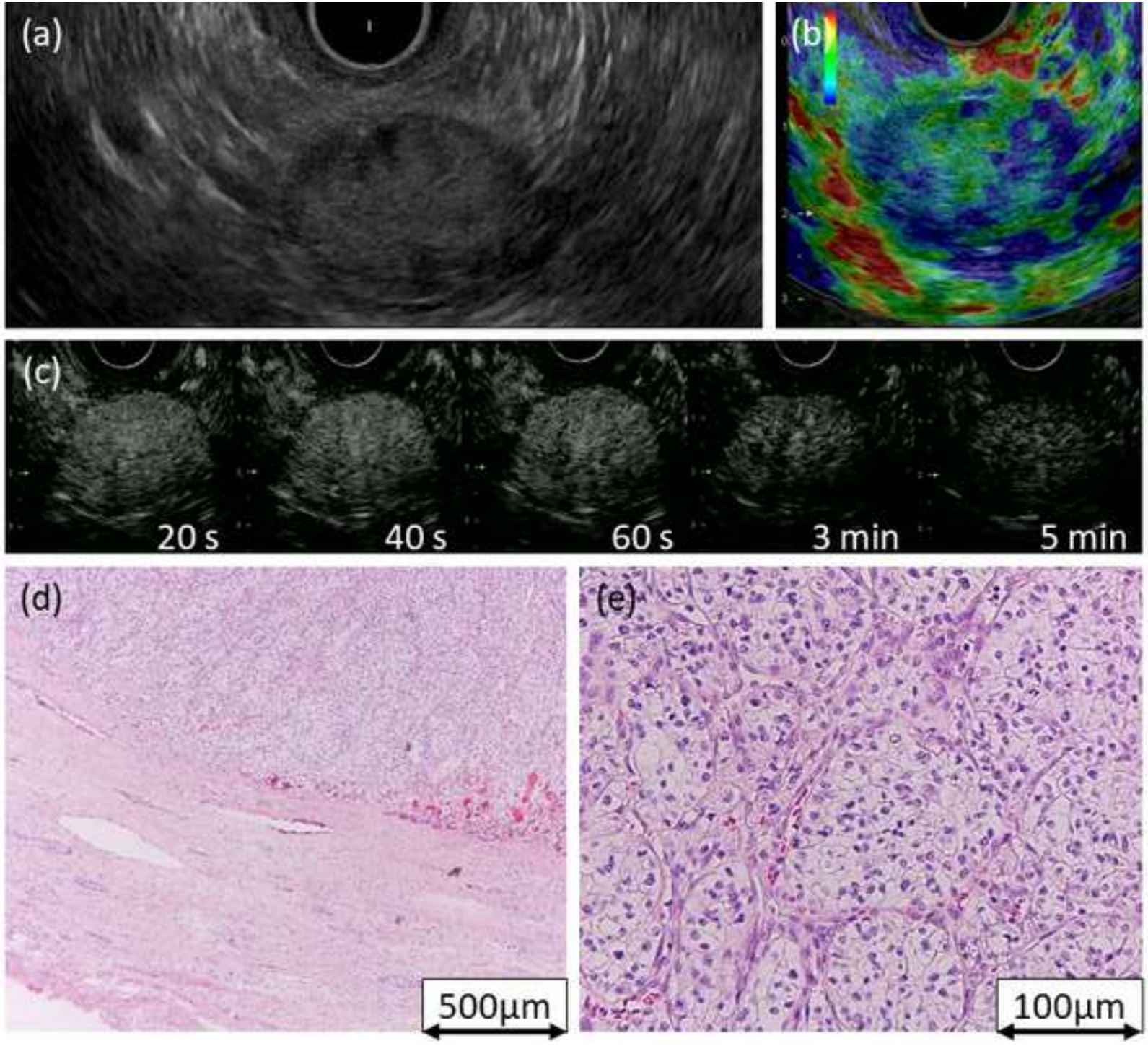

Figure